ELSEVIER

Rotation and phase-shift operations for a charge qubit in a double quantum dot

Toshimasa Fujisawa[a,*], Toshiaki Hayashi[a], H.D. Cheong[b], Y.H. Jeong[c], Yoshiro Hirayama[a,d]

[a]*NTT Basic Research Laboratories, NTT Corporation, 3-1 Morinosato-Wakamiya, Atsugi 243-0198, Japan*
[b]*Keimyung University, Shindang-Dong, Dalseo-gu, Daegu, South Korea*
[c]*Pohang University of Science and Technology, Pohang, Kyungpook, South Korea*
[d]*CREST, 4-1-8 Honmachi, Kawaguchi 331-0012, Japan*

Abstract

Coherent time evolution of a charge qubit in a semiconductor double quantum dot is demonstrated by means of electrical pulse experiments. The qubit state is manipulated with a rectangular or tailored voltage waveform that controls the energy of the system. The initialization, rotation gate, phase-shift gate, and measurement process are sequencially performed just by changing the voltage in a short time.
© 2003 Elsevier B.V. All rights reserved.

1. Introduction

Studies on coherent quantum dynamics for single particles, such as Larmor precession and Rabi oscillation, as well as for more than two particles have been initiated from various experiments on excitation processes in atoms, and have been applied to small-scale quantum computers [1]. Nano-fabrication technology allows us to design semiconductor artificial atoms (quantum dots, QDs) and molecules (double quantum dots, DQDs), in which atomic (molecular)-like electronic states can be designed and controlled by external voltages [2–5]. The eigenstates of interacting

* Corresponding author. Tel.: +81-46-240-3449; fax: +81-46-240-4727.

E-mail address: fujisawa@will.brl.ntt.co.jp (T. Fujisawa).

electrons in quantum dots and the transitions between them can be well understood in terms of atomic physics language. These artificial atoms (molecules) may have advantages for flexible control on their states and for large-scale integration. At least, it has been demonstrated that stationary eigenstates can be tailored by adjusting static gate voltages. In order to test their potential for application to quantum information technology, coherent manipulations of non-stationary superposition state are required.

Here, we describe electrical manipulation of a charge qubit in a DQD in the Coulomb blockade regime. The qubit state is manipulated by applying a rectangular or tailored voltage pulse between the source and drain electrodes. The qubit state is effectively initialized by injecting an electron into one of the localized states. The rotation gate, which

modulates the population of each QD, is obtained by adjusting the system at the resonant tunneling condition. The phase-shift gate, which gives a phase difference between the computational bases, is executed at an off-resonant condition in a very short time. Finally, the qubit state is measured by using a tunneling process.

2. Charge qubit in a DQD

We consider a DQD (left and right dots) connected to the source and drain electrodes in series (see Fig. 1(a)). The electrical current, which flows through the DQD via three tunneling barriers, is strongly affected by the on-site and inter-dot Coulomb interactions. In the weak coupling regime, finite current is only observed when all the tunneling processes through three tunneling barriers are allowed. Under an appropriate condition, where the inter-dot tunneling is allowed but tunneling into and out of the DQD is blocked, the DQD is effectively isolated from the electrodes, which are required for the initialization and measurement processes. In this case, we can consider two charge states, in which an excess electron occupies the left dot or the right dot. In practice, each charge state involves many-body ground and excited states due to orbital and spin degrees of freedom. When the energies E_L and E_R, respectively, for two particular states $|L\rangle$ and $|R\rangle$, are energetically close to each other and the excitation to other states can be neglected, the system can be approximated by a two-level system (qubit), which is more convenient for quantum computing applications. It should be noted that $|L\rangle$ and $|R\rangle$ can be any excited state of each QD, if the population of other states can be neglected. We chose one of the excited state resonances in the experiments. The system is characterized by the energy offset $\varepsilon \equiv E_R - E_L$ and interdot tunneling, whose energy splitting is Δ. The effective Hamiltonian is

$$H = \frac{1}{2}\varepsilon\sigma_z + \frac{1}{2}\Delta\sigma_x, \tag{1}$$

where σ_x and σ_z are the Pauli matrices for pseudo-spin as bases of $|L\rangle$ and $|R\rangle$. The eigenstates of the system are bonding and anti-bonding states, whose energies (E_a and E_b) are schematically shown in Fig. 1(b). The system can also be mapped onto the Bloch sphere of
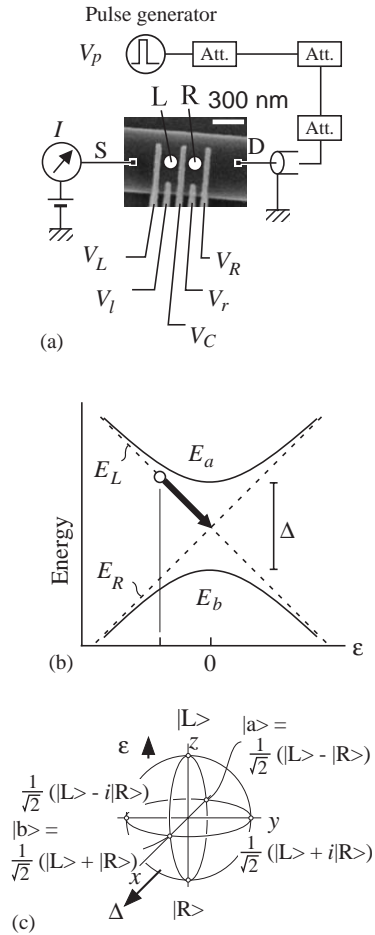

Fig. 1. (a) Schematic of the measurement setup and a scanning microscope image of the sample. Etching (upper and lower dark regions) and negatively biased gate electrodes defined a double quantum dot (L and R) between the source (S) and drain (D). (b) Energy levels of the bonding (E_b) and anti-bonding (E_a) states, which are the eigenstates during the manipulation, and localized states (E_L and E_R) during initialization. (c) The Bloch sphere of the pseudo-spin qubit.

a pseudo-spin in a fictitious magnetic filed (ε and Δ), as shown in Fig. 1(c).

The DQDs used in this work are defined by metal gates on top of a GaAs/AlGaAs heterostructure with a two-dimensional electron gas (2DEG). Each dot contains about 25 electrons with on-site charging energy $E_c \sim 1.3$ meV. The interdot charging energy is $U = 200$ μeV. The qubit parameters, ε and Δ, and tunneling rates, Γ_L and Γ_R, respectively, for left and right

barriers, can be roughly estimated from elastic tunneling current and tuned by gate voltages [4,6]. In the region of interest, $|\varepsilon| \lesssim 50$ µeV and $\Delta = 5$–10 µeV is smaller than U and smaller than the typical level spacing of each dot, ~ 100 µeV, where the system can be approximated by a two-level system. The experiments were performed at lattice temperature of $T_{\text{lat}} \lesssim 20$ mK in a magnetic field of 0.5 T applied perpendicular to the 2DEG. The effective electron temperature, which is estimated from the line width of a single electron tunneling current through a single quantum dot, remained at $T_{\text{elec}} \sim 100$ mK, probably due to high-frequency noise. In the following experiment, we only changed ε in a short time with a quasi-constant Δ.

A rectangular voltage pulse was applied to the drain electrode via a low-distortion coaxial cable. The pulse switches the source–drain bias voltage between high (600 µV) and zero. Due to the mutual coupling between the QDs and electrodes, the pulse also shifts the energy offset from $\varepsilon = \varepsilon_0$ to ε_1 by $\varepsilon_1 - \varepsilon_0 \sim 40$ µeV. We design the pulse sequence that performs initialization, coherent manipulation, and measurement in the following way. Although the basic idea is borrowed from experiments on a superconducting island [7], our qubit is effectively isolated from the electrode during the manipulation, while it is influenced by strong decoherence during initialization.

3. Rotation gate

The rotation gate is obtained by applying a rectangular voltage waveform. Fig. 2(a) shows a typical waveform (pulse length of 400 ps) for the rotation gate. The actual waveform at the sample is deformed by the frequency-dependent loss of the coaxial cable.

For initialization, we applied a relatively large source–drain voltage, $V_{\text{sd}} \sim 600$ µV (Fig. 2(b)). We also adjusted the gate voltages so that $|L\rangle$ and $|R\rangle$ would be out of resonance in the transport window ($\mu_S > E_L > E_R > \mu_D = \mu_S - eV_{\text{sd}}$, $\varepsilon = \varepsilon_0 \sim -40$ µeV). Elastic and inelastic current flows through the DQD, but the current is always limited by the central barrier when the outer tunneling barriers have higher tunneling rates ($\hbar\Gamma_L \sim \hbar\Gamma_R \sim 30$ µeV $> \Delta$, $\hbar\Gamma_i$), where Γ_i is the inelastic tunneling rate between the two dots ($\hbar\Gamma_i \sim 0.1$–4 µeV). In this case, the DQD is effectively initialized to $|L\rangle$.

For coherent manipulation, we immediately change the source–drain voltage to zero, and shift the energy offset to $\varepsilon = \varepsilon_1 \sim 0$ (Fig. 2(c)). In this case, the inter-dot charging energy prevents electrons tunneling in and out of the DQD within the first-order tunneling process, and no current flows through the DQD. The qubit is effectively isolated from the electrodes. Therefore, the system is well approximated by Eq. (1). The rise time of voltage pulse was about 100 ps, which is fast enough to change the system non-adiabatically. The system first prepared in $|L\rangle$, goes back and forth between the two dots. In the Bloch sphere representation, the pseudo-spin state rotates about the total fictitious magnetic field (Lamor precession). We maintained zero bias voltage for a duration, $t_{\text{p}} = 80$–2000 ps.

Then, the large bias voltage is restored for measurement process (Fig. 2(d)). The large tunneling rate ($\hbar\Gamma_L$, $\hbar\Gamma_R$) and off-resonant condition effectively ceases the coherent precession, and provides a strong measurement. If the electron ends up in the right QD, it tunnels out to the right electrode and contributes to the excess pulse-induced current. If the electron end up in the left dot, however, it cannot do so. The system automatically goes to the initial state after waiting longer than $\Gamma_L^{-1} + \Gamma_R^{-1}$.

In practice, we repeatedly apply many pulses with repetition time $t_{\text{rep}} = 10$ ns $\gg \Gamma_L^{-1} + \Gamma_R^{-1}$, and measured the average DC current, I. In order to improve the signal-to-noise ratio, we employed lock-in amplifier technique to measure the pulse-induced current, I_{p}, by switching the pulse train on and off at a modulation frequency of 100 Hz. We evaluate the average number of pulse-induced tunneling electrons, $\langle n_{\text{p}} \rangle = I_{\text{p}} / e f_{\text{rep}}$.

Fig. 3(b) shows a color plot of the pulse-induced current I_{p} as a functions of pulse length t_{p} and energy offset ε_1 during the manipulation. In this experiment, ε_0 and ε_1 were simultaneously swept by changing a gate voltage, V_R. The condition $\varepsilon_0 = 0$ was determined at the resonant tunneling peak in the absence of the pulse, while the condition $\varepsilon_1 = 0$ was determined at the current peak in I_{p} for $t_{\text{p}} > 1$ ns. Clear oscillations were observed in the time domain at $\varepsilon_1 \sim 0$. The trace at $\varepsilon_1 = 0$ is also shown in Fig. 3(a). The oscillation can be fitted very well with the exponential decay of the cosine function and a linearly decreasing term,

$$\langle n_{\text{p}}(t_{\text{p}}) \rangle \simeq A \exp(-t_{\text{p}}/T_2) \cos(\Omega t_{\text{p}} + \alpha) - \Gamma_i t_{\text{p}}, \quad (2)$$
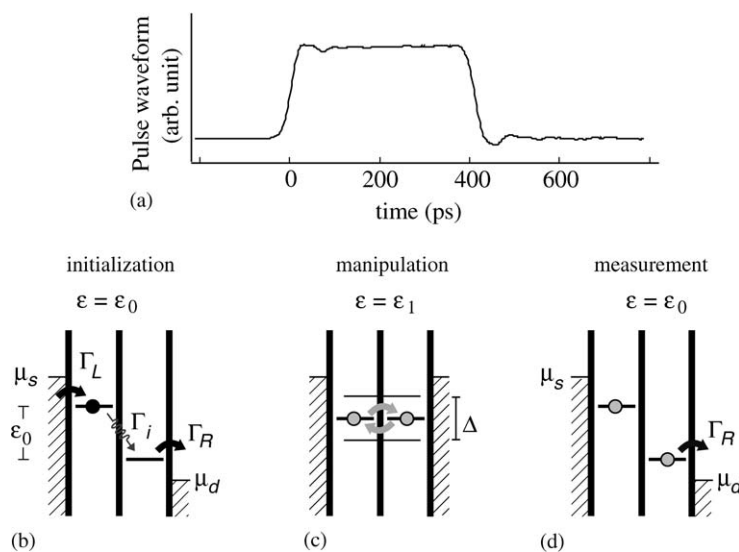
Fig. 2. (a) The rectangular pulse waveform used for the rotation gate. The rise time of the pulse was about 40 ps at the pulse generator, but degraded to about 100 ps at the sample. Energy diagrams of the DQD during (b) initialization, (c) coherent oscillation, and (d) measurement process.
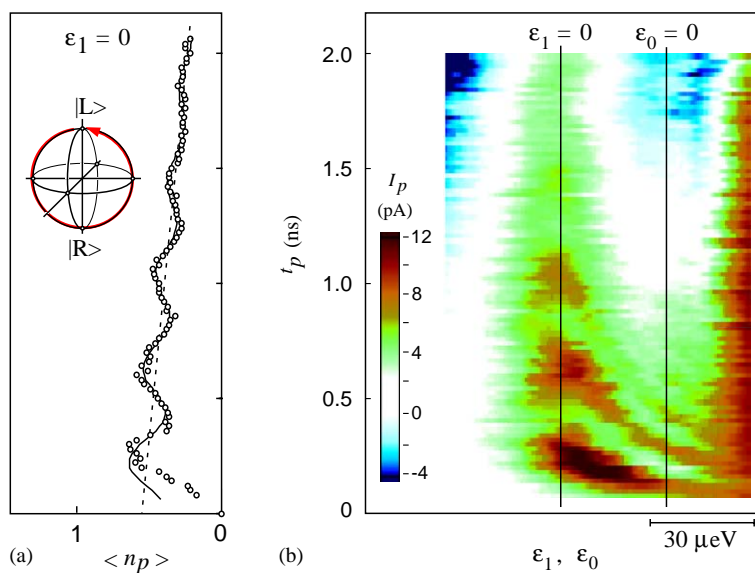

Fig. 3. (a) The pulse-induced tunneling electrons, $\langle n_p \rangle$. The solid line is a damped cosine function with a linearly decreasing term, which is fitted to the data. (b) Color plot of the pulse induced current, I_p.

except for the rise time of the voltage pulse ($t_p < 100$ ps). The amplitude of the oscillation, $A \sim 0.3$, which is smaller than unity, may arise from the finite rise time of the pulse as well as the non-ideal

initialization and measurement processes. The small phase shift α might also arise from the finite rise time. The last term corresponds to the reduction of the inelastic tunneling current, which only flows during

high V_{sd}. Γ_i obtained from this fitting almost agrees
with the inelastic DC current amplitude, indicating the
validity of the isolated quantum state during the ma-
nipulation. We determined the oscillation frequency
$\Omega/2\pi$ to be ~ 2.3 GHz and the decoherence time T_2 to
be ~ 1 ns from the fitting. The $\hbar\Omega$ should correspond
to the energy splitting of the bonding and antibonding
states, $\hbar\Omega = \sqrt{\varepsilon_1^2 + \Delta^2}$, from which we can determine
Δ.

The oscillation pattern in Fig. 3(b) shows that the
amplitude and period decreases when ε_1 is out of the
resonance. The asymmetry of the current profile at
around $\varepsilon_1 = 0$ arises from the finite rise time of the
voltage pulse [7]. A clear oscillation appears if the
transient from ε_0 to ε_1 crosses the resonant condition
(i.e., $\varepsilon_0 \lesssim 0 \lesssim \varepsilon_1$).

We can control Δ to be from 6 to 12 μeV by chang-
ing the central gate voltage, V_C, as shown in Fig. 4.
However, the decoherence time is always limited to
about 1 ns. Possible decoherence mechanisms will be
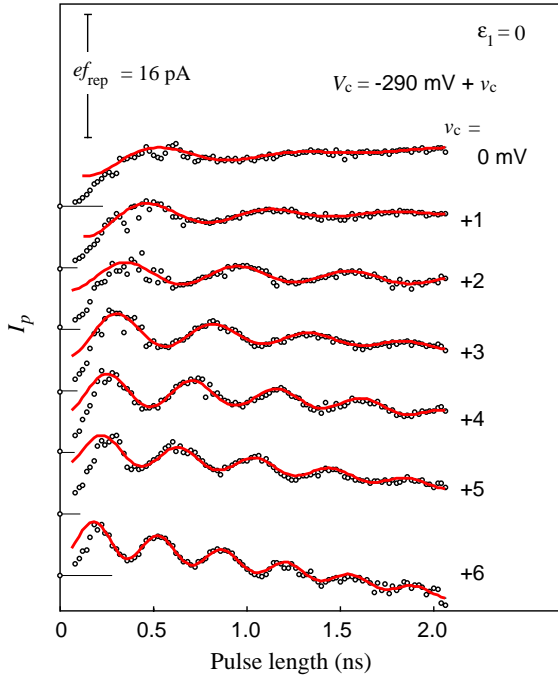discussed in a separate paper [8].

Fig. 4. The pulse-induced current, I_p, observed for different central
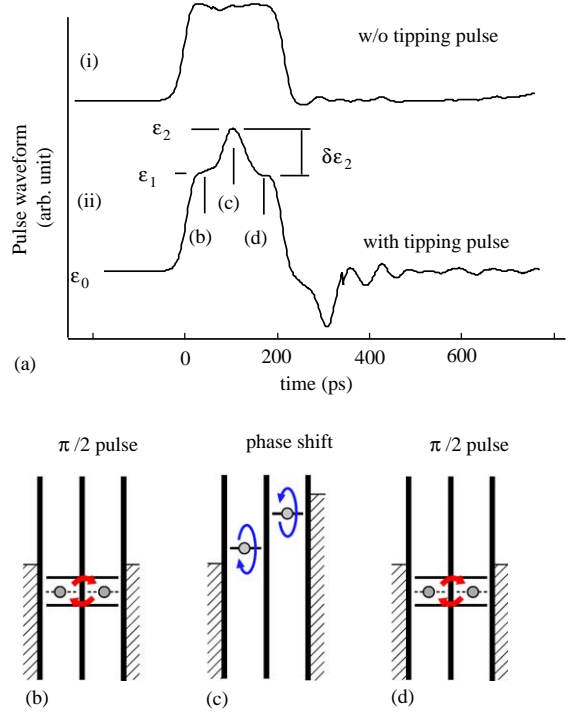gate voltages.

Fig. 5. (a) The pulse waveform used for the phase-shift gate. The
original π pulse without a tipping pulse (i) and with a tipping
pulse at the center of the π pulse (ii). Energy diagrams of the
DQD during (b) the first $\pi/2$ pulse, (c) the phase-shift gate, and
(d) the second $\pi/2$ pulse.

4. Phase-shift gate

The phase-shift gate is obtained by applying a large
source–drain voltage during the manipulation to shift
the energy offset to $\varepsilon = \varepsilon_2$. Leaving a state at $\varepsilon_2 \gg \Delta$ for
a specific time t_ϕ produces a phase shift $\phi = \varepsilon_2 t_\phi/\hbar$ [9].
Fig. 5(a) shows the pulse waveform for demonstrat-
ing the phase-shift gate. The rectangular waveform (i)
with pulse length of 200 ps works as a π pulse for
$\Delta = 10$ μeV at $\varepsilon_1 = 0$. A single sharp pulse, which
we refer to as a tipping pulse, is superimposed at the
center of the main pulse [see waveform (ii)]. When
we neglect non-ideal factors, the first half of the rect-
angular pulse ($\pi/2$ pulse, Fig. 5(b)) puts the system
in the superposition state $\frac{1}{\sqrt{2}}(|L\rangle - i|R\rangle)$. The tipping
pulse gives a phase shift ϕ, and thus the state becomes
$\frac{1}{\sqrt{2}}(|L\rangle - i\exp(i\phi)|R\rangle)$ (Fig. 5(c)). The second half
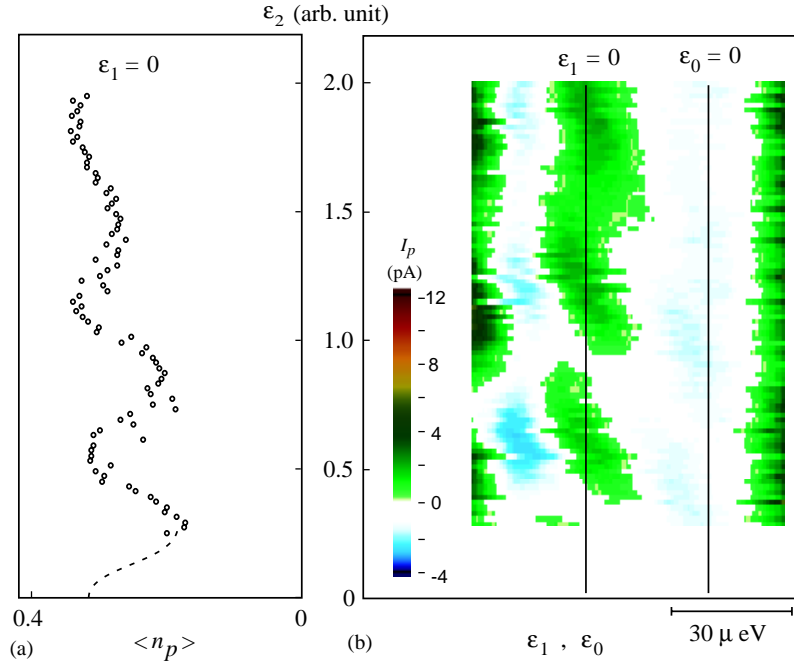of the pulse [$\pi/2$ pulse, Fig. 5(d)] changes the system

Fig. 6. (a) The pulse-induced tunneling electrons, $\langle n_p \rangle$, for demonstrating the phase-shift gate. The dashed curve is a guide for the eye. (b) Color plot of the pulse induced current, I_p.

to $\frac{1}{2}((1 - e^{i\phi})|L\rangle + (1 + e^{i\phi})|R\rangle)$. Therefore, the probability of finding the system in $|R\rangle$ oscillates in ϕ.

However, in our experimental scheme, the high ε_2 requires a large source–drain voltage, which can break the Coulomb blockade condition and induce strong decoherence from the tunneling. Therefore, we minimize the time duration t_ϕ for the phase-shift gate, and change ε_2 to control the phase shift. The tipping pulse is prepared by making a derivative of another rectangular pulse of the same length. This gives an additional negative pulse just after the main pulse. We believe this negative pulse does not affect the following measurements very much.

Fig. 6(b) shows the color plot of the pulse-induced current when ε_0 and ε_1 are simultaneously swept by changing V_R (horizontal axis) and $\delta\varepsilon_2 = \varepsilon_2 - \varepsilon_1$ are changed (vertical axis). The oscillations observed at $\varepsilon_1 = 0$ (Fig. 6(a)) indicate the phase-shift gate operation. The amplitude slightly decays with increasing $\delta\varepsilon_2$, although pulse width remained constant. The maximum $\delta\varepsilon_2$ (2.0 arbitrary unit in Fig. 6) corresponds to about 5 mV in the source–drain voltage, which is

much greater than the charging energy of the dots. Additional decoherence might come from enhanced tunneling rates via other excited states at high ε_2.

5. Summary

We have successfully observed coherent charge oscillations of a charge qubit in a double quantum dot. Although the quality of the oscillation is not very good due to decoherence, our observation could stimulate studies on coherent dynamics in semiconductor quantum dots.

References

[1] M.A. Nielsen, I.L. Chuang, Quantum Computation and Quantum Information, Cambridge University Press, Cambridge, 2000.
[2] S. Tarucha, D.G. Austing, T. Honda, R.J. van der Hage, L.P. Kouwenhoven, Phys. Rev. Lett. 77 (1996) 3613.

[3] T.H. Oosterkamp, T. Fujisawa, W.G. van der Wiel, K. Ishibashi, R.V. Hijman, S. Tarucha, L.P. Kouwenhoven, Nature 395 (1998) 873.

[4] T. Fujisawa, T.H. Oosterkamp, W.G. van der Wiel, B.W. Broer, R. Aguado, S. Tarucha, L.P. Kouwenhoven, Science 282 (1998) 932.

[5] T. Fujisawa, D. G. Austing, Y. Tokura, Y. Hirayama, S. Tarucha, Nature 419 (2002) 278.

[6] W.G. van der Wiel, S. De Franceschi, J.M. Elzerman, T. Fujisawa, S. Tarucha, L.P. Kouwenhoven, Rev. Mod. Phys. 75 (2003) 1.

[7] Y. Nakamura, Yu.A. Pashkin, J.S. Tsai, Nature 398 (1999) 786.

[8] T. Hayashi, T. Fujisawa, H.D. Cheong, Y.H. Jeong, Y. Hirayama, Phys. Rev. Lett. 91 (2003) 226804.

[9] Y. Nakamura, Yu.A. Pashkin, T. Yamamoto, J.S. Tsai, Phys. Rev. Lett. 88 (2002) 047901.